JOURNAL OF CATALYSIS 101, 123–131 (1986)

Structure Effects in Ethane Hydrogenolysis on Rh/SiO_2 Catalysts[1]

C. LEE AND L. D. SCHMIDT

Department of Chemical Engineering and Materials Science, University of Minnesota, Minneapolis, Minnesota 55455

Received February 15, 1986; revised April 18, 1986

The effects of oxidation–reduction cycling on the morphology, surface composition, metal surface area, and kinetics of ethane hydrogenolysis on Rh particles on SiO_2 have been studied by hydrogen chemisorption, kinetics in a differential flow reactor, transmission electron microscopy (TEM), and X-ray photoelectron spectroscopy (XPS). When ~150-Å-diameter Rh particles are oxidized at 500°C and then reduced in H_2 at 250°C, the activity increases by up to three orders of magnitude. Heating progressively up to 650°C produces a decrease in activity to nearly its original value. Hydrogen uptake shows only a factor of less than 3 increase in metal surface area associated with the redispersion and sintering following oxidation and reduction. XPS confirms total oxidation by 500°C and reduction by 150°C. TEM shows that particles spread on the SiO_2 surface upon oxidation and form clusters of smaller Rh particles upon low-temperature reduction. These large activity changes appear to be associated with morphological changes in types and distribution of active sites on the metal surface. These transformations can be produced reversibly by successive oxidation–reduction treatments, and structures can be metastable for long times under reaction conditions.

INTRODUCTION

The relation between catalytic properties and the microstructure of a metal catalyst is a basic issue which is usually addressed only indirectly by comparing properties of catalysts with preparation conditions or loading. The influence of dispersion (or particle size) on the specific activity of ethane hydrogenolysis on various metals has been reported by several research groups. Yates and Sinfelt (*1*) investigated the variation of catalytic properties with the state of dispersion for a series of Rh/SiO_2 catalysts and reported a maximum of the specific activity for ethane hydrogenolysis at a dispersion near 50%. They reported that a 48% dispersion catalyst was 33 times more active than an 8.6% dispersion catalyst at 253°C. Martin and Dalmon (*2*) studied ethane hydrogenolysis over silica-supported nickel catalysts and showed that increasing nickel particle size by thermal sintering in hydrogen results in a large decrease of specific activity. They found a maximum in specific activity with an average Ni particle size around 50 Å. The variation of activity was about a factor of 20 among samples which agrees with data reported by Carter *et al.* (*3*).

Goodman (*4*) measured the specific rates of ethane hydrogenolysis over the (100) and (111) planes of nickel. He observed that the (111) surface is less active toward hydrogenolysis than the (100) surface by about three orders of magnitude at 230°C. He reported a difference of 15 kcal/mol in activation energy between these crystal planes.

In all of these studies high-area supported catalysts were prepared by reduction in a hydrogen stream with the temperature range between 400 and 650°C. Yates and Sinfelt (*1*) reduced their catalyst samples at 450°C for 2 hr or 400°C for 16 hr. Martin and Dalmon's (*2*) Ni/SiO_2 catalyst samples were obtained by reduction at 650°C for 15 hr. The exposed faces of the metal particles were suggested to be mostly low index planes (*5*) such as (111), (100),

[1] This work partially supported by NSF under Grant CPE 8214048.

0021-9517/86 $3.00

and (110) under these conditions. However, supported metal catalysts are exposed to various oxidizing and reducing gas atmospheres during operation and regeneration. From the results of TEM studies on model catalysts which have been conducted in this and other laboratories, it is clear that microstructures of small particles are altered by different gas environments, and this may play an important role in determining the performance of a catalyst. On the other hand, heterogeneous reactions take place only on the top monolayer of the particle surface, and it is therefore necessary to correlate the reactivity of the catalyst with its morphology and surface composition. This characterization can only be obtained with electron microscopy coupled with surface sensitive spectroscopies.

Recently, transmission electron microscopy (TEM) studies using model catalysts have revealed various types of behavior of supported metal particles in gaseous environments (*6–11*). It has been shown that alternate oxidation and reduction can lead to a transformation in morphology of supported particles, i.e., redispersion. Previously, we observed the redispersion of Rh and Ni on silica and alumina (*9–10*) by oxidation and low-temperature H_2 reduction. Nakayama, *et al.* (*11*) showed that silica- and alumina-supported Ni particles can be redispersed by repeated oxidation–reduction treatments.

In a recent study (*10*), we correlated the kinetics of CO hydrogenation on Ni/SiO_2 with particle microstructure. We observed that when Ni particles (~4% dispersion, ~250 Å diameter) were oxidized at 460°C and then reduced in H_2 at 300°C, hydrogen chemisorption areas increased by a factor of 1.3 while methanation activities decreased by a factor of 2.0. Heating progressively up to 650°C produced a decrease in surface area and an increase in methanation activity to nearly the previous values. XPS confirmed total oxidation and reduction of Ni by 350°C. TEM showed that particles spread on the SiO_2 upon oxidation and formed clusters of smaller Ni particles upon low temperature reduction, a clear correlation of reactivity with catalyst microstructure.

The present study aims to elucidate the correlation between Rh particle microstructure and ethane hydrogenolysis kinetics. We examine the effects of repeated oxidation–reduction on the performance of Rh particles on amorphous SiO_2. We show using TEM that oxidation and reduction of Rh produces dramatic changes in the particle morphology. Solid-state redispersion causes the particle surface to be very irregular upon low-temperature reduction, but high-temperature reduction transforms the morphology back to the regular shape.

EXPERIMENTAL

A flow microreactor system with about 300 mg of catalyst and an on-line HP 5793 gas chromatograph (GC) with a flame ionization detector were used to study hydrogen chemisorption and ethane hydrogenolysis kinetics. Hydrogen uptake was measured by the GC flow desorption method described by Amelse *et al.* (*12*) with a thermal conductivity detector. For kinetics measurements the conversion of C_2H_6 was kept less than 5 to 20%.

The 5% Rh/SiO_2 catalyst was prepared by impregnation of 200 m^2/g Cab-O-Sil SiO_2 to incipient wetness with an aqueous solution of $RhCl_3 \cdot 3H_2O$. The catalyst was dried overnight at 100°C and then calcined in O_2 at 800°C for 4 hr. Hydrogen (99.9995%, Matheson) was used without further purification. The reaction gas mixture was 3% ethane and 20% H_2 in helium supplied by Linde. Nitrogen carrier gas (zero gas, Matheson) in hydrogen chemisorption experiments was passed through an Oxisorb unit to remove traces of oxygen.

Planar samples for TEM were prepared by vacuum deposition of a 15- to 20-Å Rh film on a 200-Å-thick SiO_2 flake mounted on a gold grid using procedures described previously (*9*). The SiO_2 substrate was prepared by vacuum deposition of a 200-Å film

of Si on NaCl, floating Si flakes off in H_2O, catching a flake on a gold grid, and oxidizing to 800°C in air for several days. The SiO_2 formed by this procedure is planar and amorphous. TEM samples were treated in a quartz tube furnace in flowing gases. Samples were examined in a JEOL 100CX STEM. A sample could be transferred repeatedly between the STEM and quartz tube furnace so that morphological changes of individual particles could be examined.

The SiO_2 substrates used for XPS studies were prepared by air oxidizing a 1-cm disk of high-purity Si to obtain a 1000-Å-thick layer of amorphous SiO_2. The Rh film was vacuum deposited simultaneously with the TEM samples. Specimens were heated in flowing air or H_2 for 1 hr at temperatures indicated and allowed to cool to room temperature before removal. In all experiments the same sample was transferred repeatedly between the furnace and the XPS system for treatment and analysis.

X-Ray photoelectron spectra were obtained on a Perkin–Elmer Physical Electronics Model 555 system with a Mg$K\alpha$ anode ($h\nu$ = 1253.6 eV). Peak positions were always within 1 eV of tabulated positions, presumably because the high electrical conductivity of the Si core of the specimen minimized charging. Peak energies were determined relative to the Si (103.4 eV) and C (284.6 eV) peaks on the specimen.

RESULTS

Correlation of Hydrogenolysis Activity with Sequential Oxidation and Reduction Treatments

In order to investigate the effects of morphology transformation on ethane hydrogenolysis kinetics, the catalyst in the Pyrex reactor was subjected to the same sequence of treatments in situ as that used for TEM and XPS studies. After each stage of oxidation–reduction or reduction, the porous catalyst sample was brought to the desired temperature in flowing H_2 (~40 cm^3/min), the reactant (3% ethane, 20% hydrogen in helium) at a total pressure of 1 atm was introduced into the reactor at ~60 cm^3/min, and the effluent concentrations were sampled and analyzed every 10 min. Steady-state activity was obtained within 10 min at all temperatures.

Samples were first oxidized in air at 500°C and then reduced in H_2 at increasing temperatures. Figure 1 shows the rate of CH_4 production following H_2 treatment at temperatures indicated. The treatment conditions of one cycle can be described by the sequence

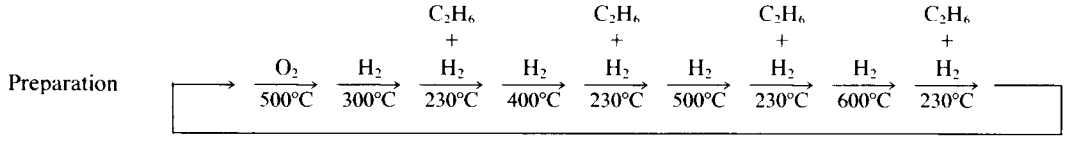

The sample was treated at each temperature for 4 hr. The activity was then measured in a steady-state flow configuration at 230°C. The activity clearly increases upon reduction at low temperatures (300 or 250°C) following oxidation at 500°C. As the temperature of H_2 treatment increases, the CH_4 rate decreases dramatically. The variation in activity is as much as three orders of magnitude.

Cyclic oxidation–reduction produces an almost reversible behavior with respect to CH_4 production rate in that reoxidation after reduction at 600°C restores activity to its previous value. Figure 1 shows results for three oxidation–reduction cycles. The activity at each stage decreased monotonically with an overall decrease by a factor of ~2 after three cycles.

Figure 2 shows Arrhenius plots for one cycle with points labeled as 1 through 5 in Fig. 1 (the third cycle). It is evident that the activity and the activation energy vary with pretreatment. The activation energy is 39

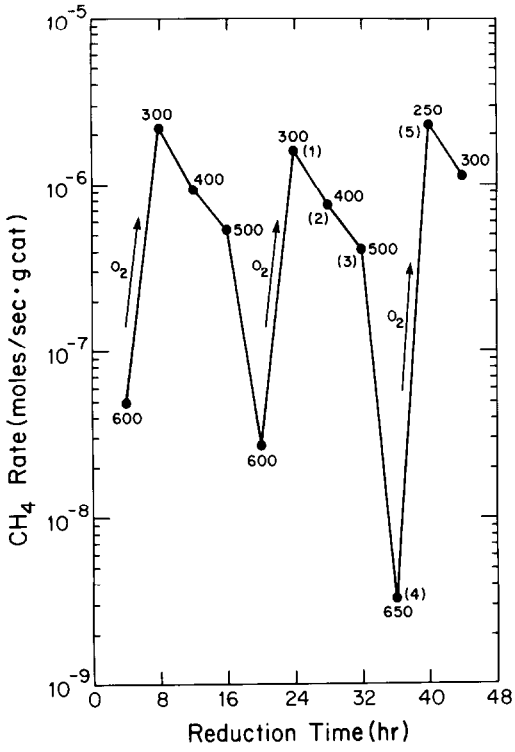

FIG. 1. Methane formation rate following oxidation–reduction. The abscissa is the total reduction time beginning with the freshly calcined sample. For each oxidation–reduction, the sample was oxidized in flowing air at 500°C for 4 hr and then reduced in H_2 for another 4 hr at the temperature indicated. Each oxidation–reduction is indicated by an O_2 and an arrow next to the line between those points. Activities were measured at 230°C with a 3% ethane, 20% H_2 in He mixture and a total pressure of 1 atm.

kcal/mol after 300°C reduction, but as the reduction temperature increases, the activation energy increases to 42 kcal/mol at 400°C and 42 kcal/mol at 500°C. However, a large change in both activity and activation energy occurred with 650°C reduction. The activation energy increased to 64 kcal/mol, 25 kcal/mol higher than after 300°C reduction. When, the catalyst was oxidized again at 500°C and reduced at 250°C, both activity and activation energy were restored (point 5).

Hydrogen chemisorption was used to determine the Rh surface area after each stage of reduction. Figure 3 shows a plot of the activation energy and preexponential factor of ethane hydrogenolysis along with the hydrogen uptake as a function of pretreatment. It is evident that the reaction activation energy and preexponential factor vary in the opposite way as the activity. With high-temperature reduction at 600 or 650°C, the activation energy and preexponential factor have the largest value and both are suppressed by oxidation–reduction. A plot of the log of preexponential factor r_0 vs activation energy E_{act} is shown in Fig. 4. All data fall on a straight line showing a strong compensation effect.

In Fig. 3c, the hydrogen uptake shows some sintering upon higher temperature reduction and redispersion upon oxidation–reduction. However, the variation is less than a factor of 3 for any treatment, much less than the change in hydrogenolysis activity.

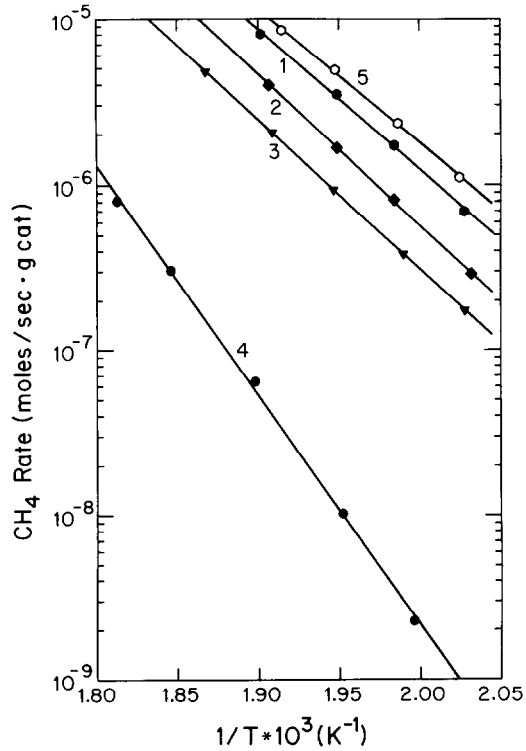

FIG. 2. Arrhenius plots for steady-state methane formation over a 5% Rh/SiO_2 catalyst, after (1) 300, (2) 400, (3) 500, (4) 650°C reduction, and (5) 250°C reduction following 500°C oxidation. Points labeled as 1–5 in Fig. 1 are the methane formation rates derived from Arrhenius plots (1)–(5).

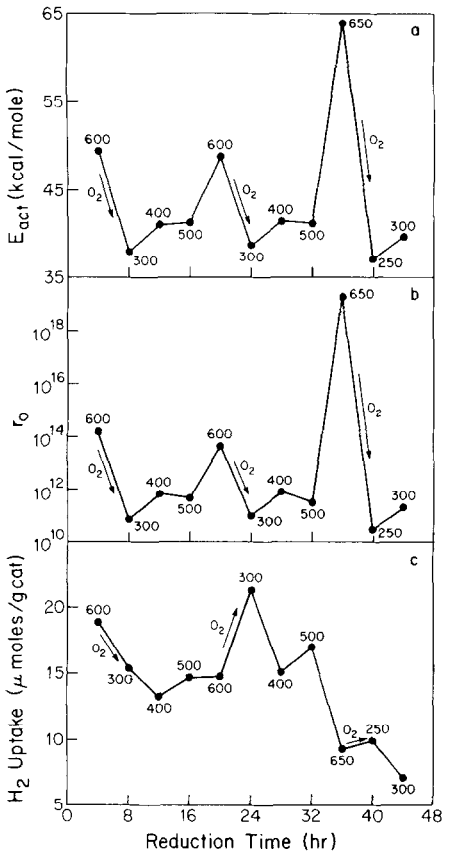

FIG. 3. Effect of reduction temperature on the performance of a 5% Rh/SiO_2 catalyst, (a) activation energy of reaction, (b) $\log_{10}$ of reaction preexponential factor, and (c) hydrogen uptake vs reduction time. Activities were measured at 230°C with a 3% ethane, 20% H_2 in He mixture at a total pressure of 1 atm.

Morphology Transformations

Figure 5 shows TEM micrographs of a specimen with a 20-Å initial loading of Rh on amorphous SiO_2 after heating in O_2 or H_2 at temperatures indicated. After heating in flowing H_2 at 600°C for 1 hr (Fig. 5a), most particles are roughly hexagonal and the smaller ones appear circular. This is typical of particles grown at high temperature in H_2. Six-sided particle outlines should be observed from a cuboctahedron (polyhedron exposing (111) and (100) planes) for most orientations with respect to the substrate.

After oxidation at 500°C (Fig. 5b), the electron diffraction pattern indicates that most of the Rh is oxidized to Rh_2O_3, leaving only a small amount of higher contrast unoxidized metal at the core of most oxide particles. All particles are observed to spread on the substrate upon oxidation. These results are identical to those described previously for oxidation of Rh on SiO_2 (9).

Figures 5c to f show micrographs of the same region following exposures to H_2 for 1 hr at successively increasing temperatures. After heating to 300°C (Fig. 5c), the oxide particles split into clusters of smaller particles which are separated by channels or cracks 5–10 Å wide. Electron diffraction at this temperature showed a weak diffuse fcc pattern and no rings of Rh_2O_3, indicating that these clusters are mostly reduced but not well crystallized. This breakup phenomenon seems to occur generally for particles of all sizes between 20 and 200 Å.

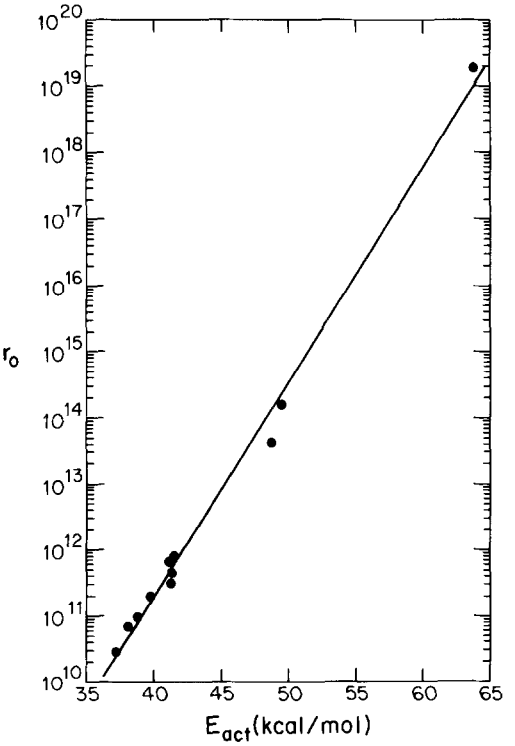

FIG. 4. Compensation effect for ethane hydrogenolysis. The $\log_{10}$ of the preexponential factor is plotted against the apparent activation energy E_{act} for data in Figs. 3a and b.

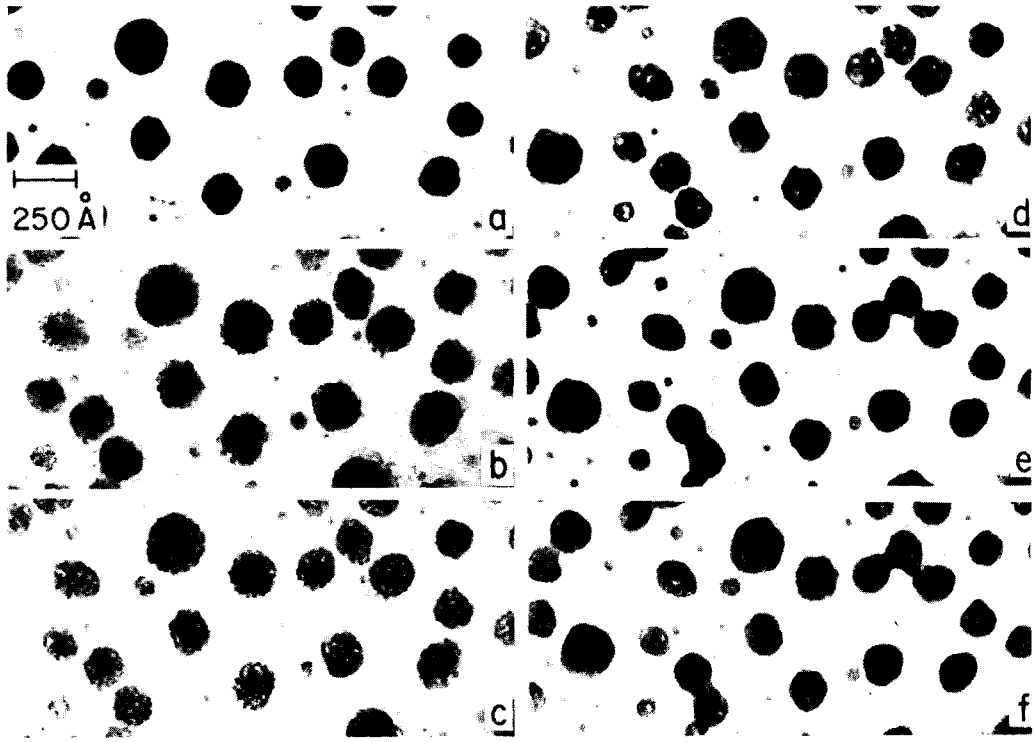

FIG. 5. Transmission electron micrographs showing the morphologies of metal and oxide particles formed by heating pure Rh on SiO_2 for 1 hr in (a) H_2 at 600°C and (b) air at 500°C. This was followed by heating in H_2 at (c) 300°C, (d) 400°C, (e) 500°C, and (f) 600°C, respectively. Splitting of metal particles occurs upon reduction of Rh_2O_3 at low temperatures.

Comparison of this micrograph with Fig. 5a shows that each original particle breaks into a cluster of smaller particles. The geometries of these particles appear irregular, and most are only 5 to 20 Å in diameter. The gaps between newly formed crystallites disappear as the temperature is increased. By 400°C (Fig. 5d) most channels are completely filled by Rh, although some large cracks are still evident. The electron diffraction pattern by 400°C showed only the sharp rings of fcc metal.

Subsequent heating of this specimen to higher temperatures in H_2 produces sintering and coalescence of Rh crystallites. Figures 5e to f show micrographs of the same region at 500 and 600°C, respectively. Coalescence occurs by growth of larger particles which finally merge with nearby particles.

Surface Oxidation States

Figures 6A and B show high-resolution XPS spectra of Rh 3*d* and O 1*s* peaks for a succession of thermal and gas treatments. Heating in H_2 at 600°C produces metallic Rh with a doublet at 307.0 and 311.8 eV, in good agreement with literature values (*13*) and with spectra of Rh foils obtained in this laboratory.

After heating to 300°C in air, small shoulders at higher binding energies of 308.6 and 313.4 eV are evident in Fig. 6A (curve b). These are confirmed to be Rh^{3+} by comparing with the spectrum of Rh_2O_3 powder on a gold foil. Upon heating at successively higher temperatures of 300 and 500°C, the size of the oxide peaks increase, and metal peaks decrease until at 500°C only Rh^{3+} peaks remain. With H_2 treatment at 150°C

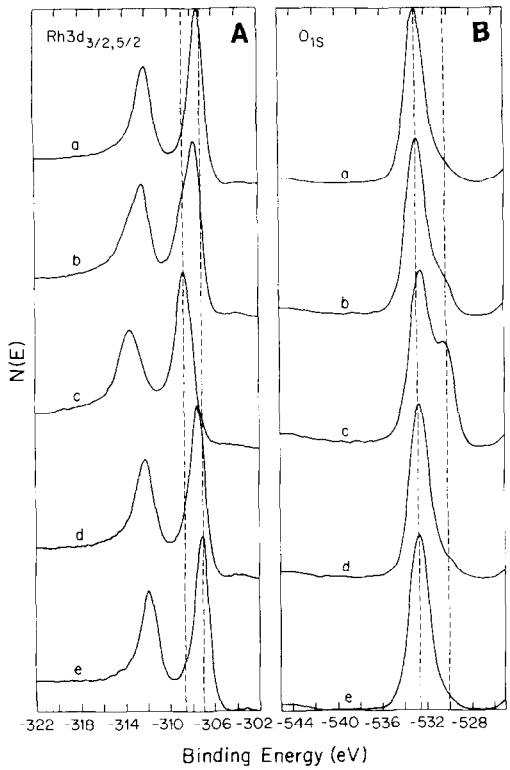

FIG. 6. (A) High-resolution XPS spectra of the Rh 3*d* doublet peaks from a planar Rh/SiO_2 sample. Spectra were obtained after treatment sequentially in (a) H_2 at 600°C, (b) air at 300°C, (c) air at 500°C, (d) H_2 at 150°C, (e) H_2 at 300°C or higher. High-binding energy peaks at 308.6 and 313.4 eV indicate Rh^{3+} from Rh_2O_3, while peaks at 307.0 and 311.8 eV are from Rh metal. (B) XPS spectra of the O 1*s* level from a planar Rh/SiO_2 sample. The sample was treated sequentially in (a) H_2 at 600°C, (b) air at 300°C, (c) air at 500°C, (d) H_2 at 150°C, (e) H_2 at 300°C and above. Treatment of Rh_2O_3 particles in H_2 at 150°C produces complete reduction to Rh metal as shown by absence of O 1*s* line at 530.0 eV.

of the sample oxidized at 500°C, curve d shows nearly complete reduction to Rh. The shoulders are barely seen and the Rh $3d_{5/2}$ peak has shifted almost back to 307.0 eV. Curve e is the spectrum with a reduction temperature higher than 300°C. It is evident that Rh_2O_3 has been totally reduced upon heating above 300°C.

The O 1*s* region is shown in Fig. 6b. The oxygen peak from SiO_2 occurs at 532.6 eV, while the peak at 530.0 eV is due to Rh_2O_3. After 600°C in H_2, there is a very small shoulder at 530.0 eV evident in Fig. 6b (curve a). This has been attributed to the oxidation at room temperature during transfer in air to the XPS chamber. As the oxidation temperature increases (curves b and c), the shoulder grows and shifts to the higher binding energy. On the other hand, the 532.6-eV peak shifts to lower energy because of overlap of peaks. The relative amount of oxygen from Rh_2O_3 decreases dramatically with H_2 reduction even at 150°C (curve d). There is no oxygen from Rh_2O_3 observed after reduction in H_2 at 300°C (curve e) and above. The sample was then reoxidized at 500°C in flowing air and reduced at or above 150°C to yield initial peak positions.

DISCUSSION

Morphology and Active Sites

To summarize these results, when an annealed Rh catalyst is subjected to oxidation followed by low-temperature H_2 treatment (1) the activity of ethane hydrogenolysis is higher by a factor of up to 1000, (2) the metal area is higher by a factor of less than 3, (3) all Rh is in the metallic state by 300°C, and (4) polyhedral particles transform into clusters. We interpret the activity change as a variation with morphology and not with variations in dispersion or chemical alteration of the surface. We emphasize that activity was measured on porous samples while TEM and XPS were on planar samples, and, while average particle sizes were identical, the correlation between reactivity and microstructure has only qualitative significance.

The dispersion is low and almost unchanged in these treatments as measured by H_2 chemisorption and by TEM. After low temperature reduction, the particle size remains at ~150 Å, but the crystal size in fact goes from 150 Å to less than 20 Å by oxidation–reduction. Thus we are not observing a dispersion effect but a crystal size effect as large crystals are transformed into clusters of small crystals.

Variations in activity with crystal size

have been attributed to variations in (1) edge and corner sites, (2) crystal planes exposed, and (3) electronic structure. We do not believe that electronic effects should be important directly (except through alterations in surface geometry) because crystals appear to be sufficiently large to possess bulk electronic structures. Substrate induced alterations also are improbable for these large clusters of particles because the substrate is not in close contact with the metal surfaces.

Site geometry therefore appears to control the activity variation. While no measurements comparing single crystal planes of Rh have been reported for this reaction, Goodman (*4*) studied ethane hydrogenolysis on Ni (100) and (111) surfaces. He observed a factor of 1000 difference between planes at 230°C with reaction activation energies of 24 and 40 kcal/mol, respectively. A transformation from (111) planes on the annealed surface to planes with a reactivity equal to the (100) plane upon oxidation–reduction would explain our rate variations.

Variations in activity may be related indirectly to chemical differences on the surfaces because different planes should have different coverages of adsorbates. Steady-state carbon coverages should be very different on different crystal planes. As an example, Caracciolo and Schmidt (*14*) used a curved nickel single crystal which exposed the [100]-[111]-[110] zone to study the crystallographic variations on the formation of surface carbon in C_2H_4 and in CO–H_2 mixtures. By exposing the crystal to ethylene at 0.1 Torr, 550 K for 300 s then annealing at 800 K under 1×10^{-9} Torr, the carbon level on the low index planes was found to be three times of that on the high index planes. However, carbon deposited from CO hydrogenation ($H_2 : CO = 3 : 1$, 2 Torr, 600 K, 10 min) showed a quite different behavior, with carbon level lower on low index planes than on high index planes.

Morphology Transformation by Oxidation and Reduction

In these experiments when a Rh particle on SiO_2 is oxidized, the oxide is observed to spread parallel to the surface upon heating at 500°C. This may arise partially from the lower density of the oxides compared to the metals, but the expansion is too large to be accounted for by this effect alone. We showed previously (*9*) that this arises from a lower interfacial energy of metal oxides compared to metal. Equivalently, one says that the metal oxide "wets" the surface while the metal does not.

As sketched in Fig. 7, a metal particle spreads over the surface of the SiO_2 upon heating in O_2 to convert it to oxide:

$$2\ Rh + 3/2\ O_2 \rightarrow Rh_2O_3. \qquad (1)$$

When this oxide is reduced back to metal

$$Rh_2O_3 + 3H_2 \rightarrow 2\ Rh + 3H_2O, \qquad (2)$$

the metal no longer wets the surface and

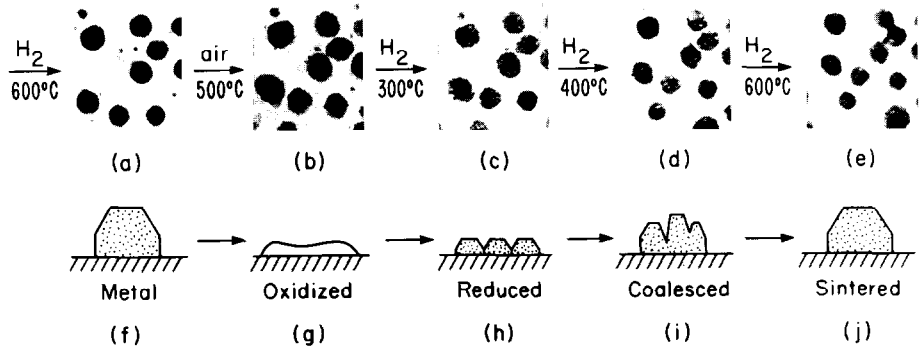

FIG. 7. TEM micrographs and sketches of idealized cross sections of Rh particles on SiO_2 treated sequentially in H_2 and O_2 at temperatures indicated.

tends to "ball up" to form a thicker particle. At low temperatures where reduction occurs but the metal atoms cannot diffuse sufficiently to coalesce, the original metal particles has been broken into a cluster of smaller metal particles as sketched in Fig. 7h. Only if heated to a temperature where surface diffusion is rapid will the cluster of metal particles coalesce back to roughly the shape of the original particle. Since surface diffusion is a thermally activated process, the surface structure will depend strongly on the treatment temperature. By 400°C (Fig. 7i), metal particles have coalesced back to roughly the shape of the original particles, but the particles still contain some imperfections. Only after reduction in excess of 500°C do particles transform completely back to single crystals.

SUMMARY

While large activity variations have been frequently noted in many catalyst systems, this appears to be one of the first observations of a large change on a *single catalyst sample*. These variations are also *reversible* in that activity can be restored by cyclic treatment.

The ability to alter catalyst behavior reversibly and predictably implies that morphological structures can be altered as needed in reactivation of real catalysts, and that it should be possible to prepare catalysts with specific activity and selectivity by appropriate microstructure alteration. The ability to achieve these capabilities reliably depends on the ability to interpret microstructural alterations produced by gas and thermal treatments in order to predict properties produced by a specific sequence of treatments.

REFERENCES

1. Yates, D. J. C., and Sinfelt, J. H., *J. Catal.* **8,** 348 (1967).
2. Martin, G. A., and Dalmon, J. A., *C.R. Acad. Sci. Paris C* **286,** 127 (1978).
3. Carter, J. L., Cusumano, J. A., and Sinfelt, J. H., *J. Phys. Chem.* **70,** 2257 (1966).
4. Goodman, D. W., *Surf. Sci.* **123,** L679 (1982).
5. Dalmai-Imelik, G., Leclercq, C., and Maubert-Muguet, A., *J. Solid State Chem.* **16,** 129 (1976); Dalmai-Imelik, G., Leclercq, C., Massardier, J., and Maubert-Muguet, A., *J. Chim. Phys.* **2,** 176 (1976).
6. Chen, J. J., and Ruckenstein, E., *J. Catal.* **69,** 254 (1981).
7. Baker, R. T. K., Prestridge, E. B., and Garten, R. L., *J. Catal.* **59,** 293 (1979).
8. Chen, M., and Schmidt, L. D., *J. Catal.* **55,** 348 (1978); **56,** 198 (1979); **60,** 356 (1979).
9. Wang, T., and Schmidt, L. D., *J. Catal.* **70,** 187 (1981); **71,** 411 (1981); **78,** 306 (1982).
10. Lee, C., Schmidt, L. D., Moulder, J. F., and Rusch, T. W., *J. Catal.* **99,** 472 (1986).
11. Nakayama, T., Arai, M., and Nishiyama, Y., *J. Catal.* **79,** 497 (1983); **87,** 108 (1984).
12. Amelse, J. M., Schwartz, L. H., and Butt, J. B., *J. Catal.* **72,** 95 (1981).
13. Mullenberg, G. E., Ed., "Handbook of X-Ray Photoelectron Spectroscopy." Perkin–Elmer Press, 1978.
14. (a) Caracciolo, R., and Schmidt, L. D., *J. Vac. Sci. Technol. A2(2),* 995 (1984); (b) *Appl. Surface Science* **25,** 95 (1986).